Phase and Energy Relaxation in an Antibonding Surface State: Cs/Cu(111)

S. Ogawa, H. Nagano, and H. Petek
Advanced Research Lab., Hitachi, Ltd., Hatoyama, Saitama, 350-0395, Japan
(Received 26 August 1998)

Electron dynamics induced by direct photoexcitation of the antibonding state on the Cs/Cu(111) surface are studied by interferometric time-resolved two-photon photoemission. Femtosecond resolution pump-probe correlation measurements indicate phase and energy decay, respectively, on 15 and 50 fs time scales for the Cs antibonding state at 33 K. Both the polarization and phase dynamics are nonexponential and strongly temperature dependent. The energy dependence of the antibonding state population dynamics is consistent with Cs photodesorption. [S0031-9007(99)08606-8]

PACS numbers: 73.50.Gr, 78.40.Kc, 79.60.–i

Energy and phase relaxation times of electronically excited states of atoms and molecules adsorbed on solid surfaces are important for many physical phenomena including surface scattering, photon and electron stimulated desorption, surface sputtering, and surface photochemistry [1]. According to the Menzel-Gomer-Redhead (MGR) model [2,3], photodesorption occurs when an adsorbate is excited to a dissociative antibonding or affinity state, if the nuclear motion along the reaction coordinate can compete with the electronic deexcitation. Typically, electronic quenching of adsorbates on metal surfaces occurs on a $\ll$10 fs time scale [4–6], which has prevented direct, real-time observation of surface photochemical reactions.

Alkali atom-metal surface chemisorption is a model system of practical importance in thermionic emission and promotion or poisoning in catalysis [7]. Near a metal surface, alkali atoms experience a repulsive interaction of the valence electron with the induced image charge of the ionic nuclear core. As the atom-surface distance is decreased, the valence electrons shift upward in energy and hybridize with those of the substrate into bonding and antibonding states [8–10]. Nordlander and Tully have calculated orbital-dependent energies and electron transfer rates of $\leq$2 fs for Cs at 3.01 Å (Cu-Cs bond length [11]) above a jellium surface [8]. In agreement with theory, an unoccupied antibonding state having a linewidth $\Gamma = 350$ meV at 300 K, which implies a lifetime τ of 2 fs according to the Heisenberg relation $\Gamma\tau = \hbar$, has been observed in inverse and two-photon photoemission (2PP) spectra of alkali metals on copper [12–14]. However, in a recent study of Cs/Cu(111), Bauer *et al.* measured a significantly longer lifetime of 11 fs by time-resolved photoemission [14], implying that Γ has significant contributions from inhomogeneous broadening and/or quasielastic [e.g., electron-phonon (e-p)] scattering. To address this contradiction and to gain a deeper understanding of the bonding, and electronic relaxation of alkali atoms on metal surfaces, it is necessary to determine both the phase and energy relaxation times of the antibonding state on Cs/Cu(111). In this Letter, the electronic relaxation is measured by the interferometric time-resolved two-photon photoemission (ITR-2PP) technique [15,16], thus providing a direct method to study the MGR photodesorption.

The ITR-2PP experiment and data evaluation method are described elsewhere [16]. Briefly, frequency-doubled light from a Ti:sapphire laser ($h\nu = 3.08$ eV; 13 fs intensity pulse width) is split into equal pump and probe pulses in a stabilized, scanning Mach-Zehnder interferometer. The pump-probe delay is scanned by $\pm$150 fs with an accuracy of $<\lambda/25$ corresponding to 5×10^{-17} s for repetitive scans. The pulses are focused collinearly to a spot of 80 μm on the sample, which is held in an ultrahigh vacuum (UHV) chamber (base pressure: $<5 \times 10^{-11}$ Torr). The p-polarized light incident at 30° from the surface normal excites 2PP, which is measured as a function of energy at $k_{\parallel} = 0$ with a hemispherical electron energy analyzer (5° angular, and 30 meV energy resolution). The 2PP spectra are measured with single-pulse excitation. Electronic relaxation rates are obtained from interferometric two-pulse correlation (I2PC) measurements, where the 2PP current is monitored at a specific energy as a function of the pump-probe delay. The Cu(111) surface is cleaned by a cyclic procedure of Ar^+ sputtering (500 V) and annealing at 700 K. The sample temperature is set between 33 and 300 K by a He closed-cycle refrigerator/heater combination. The Cs is evaporated onto a room temperature Cu(111) surface from a SAES getter while maintaining the UHV chamber pressure in the 10^{-10} Torr range. The change in the work function Φ is used to calibrate the Cs coverage [17].

A clean Cu(111) surface has a projected L band gap extending from the $L_{2'}$ point at -0.85 eV to the L_1 point at 4.08 eV, which supports a Shockley-type surface state (SS) with an energy of -0.39 eV at $k_{\parallel} = 0$ [18]. The low lying orbitals of Cs interacting with the Cu(111) surface hybridize with the SS and the sp band of copper to form partially occupied bonding (B) and unoccupied antibonding (A) states [9,10]. B is difficult to observe in photoemission spectroscopy due to its broad width and s-like orbital character [9]; however, A is readily detected in 2PP at 3.1 eV in the zero Cs coverage limit [14]. An increase in Cs coverage results in a characteristic decrease of Φ, which modifies the image potential, and

therefore decreases the energies of A and SS [13,17,19]. Therefore, direct SS $\rightarrow A$ excitation is possible by tuning the transition into resonance with the excitation light by means of the Cs coverage.

The 2PP spectra for near resonant SS $\rightarrow A$ excitation in Fig. 1 show interesting features that may be relevant to the electronic quenching of A. Two peaks labeled as SS and A are assigned to 2PP from SS and via the intermediate state A, respectively. The energy of the SS $\rightarrow A$ resonance and linewidths of both peaks decrease with temperature. The energies of Φ, A, and SS shift by -0.28, -0.19, and $+0.18$ meV/K, respectively, while, for clean Cu(111), Φ shifts by -0.10 meV/K. Thus, the magnitude of $\frac{d\Phi}{dT}$ for Cs/Cu(111) appears to be anomalous. While thermal vibrations determine $\frac{d\Phi}{dT}$ for a clean metal surface, the larger value for Cs/Cu(111) may also reflect a thermal distribution of Cs adsorption sites. Although the atop site is energetically favored [11], a surface-extended x-ray absorption fine-structure study of K/Cu(111) shows that alkali atoms are highly mobile and populate hollow sites even at 65 K [20]. A longer, more ionic Cu-Cs bond in a hollow site, as compared with an atop site [20], may produce a larger surface dipole and, therefore, a larger change in Φ *per* adsorbate. Thus, depopulation of hollow sites at low temperature should increase Φ. The high mobility and distribution of Cs in two sites may also contribute to the shift and width of A, and affect the electronic relaxation. In addition, energy of Φ and A increases with time as a result of irradiation with 3.08 eV light providing evidence of the photodesorption of Cs atoms, which is well documented for K/graphite [21,22]. The Cs atoms are depleted over the entire surface rather than just the irradiated area, confirming their high mobility even at 33 K.

Figure 2(a) shows I2PC scans for 0.11 monolayer (ML) Cs/Cu(111) at 33 K near the SS $\rightarrow A$ resonance. The I2PC data reflect the phase and energy relaxation when a three-level system is coupled by two-photon absorption, as shown in Fig. 2(b). One- and two-photon excitation induces transient linear and nonlinear (quadratic) polarization. Coherent interaction of the electric field of the probe pulse with the pump-induced polarization wave leads to interference at the excitation frequency ω and its second harmonic 2ω. The decay of the quantum mechanical phase in the excitation process is deduced by fitting the envelopes of ω and 2ω oscillations, thus providing experimental values of e-h decoherence times for the linear polarizations $T_2{}^{01}$ and $T_2{}^{12}$ (designated as $T_2{}^{\omega}$) and nonlinear polarization $T_2{}^{02}$. Once the coherent contribution is known, the incoherent intermediate state population decay is deduced from the phase averaged I2PC [16]. Fitting these envelopes to a convolution of the instrument response function with a single exponential decay gives the experimental phase and energy relaxation times in Fig. 3. However, the actual phase and energy decays are nonexponential, so this simple fitting procedure gives only a qualitative representation of the relaxation dynamics.

Interference fringes in the I2PC scans taken near the SS $\rightarrow A$ resonance in Fig. 2(a) persist for >60 fs and have energy-dependent amplitude modulation (quantum

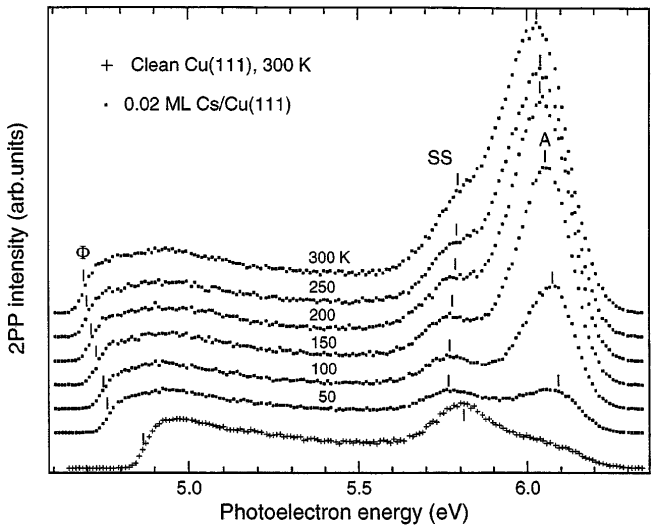

FIG. 1. Temperature dependence of 2PP spectra for 0.02 ML Cs/Cu(111).

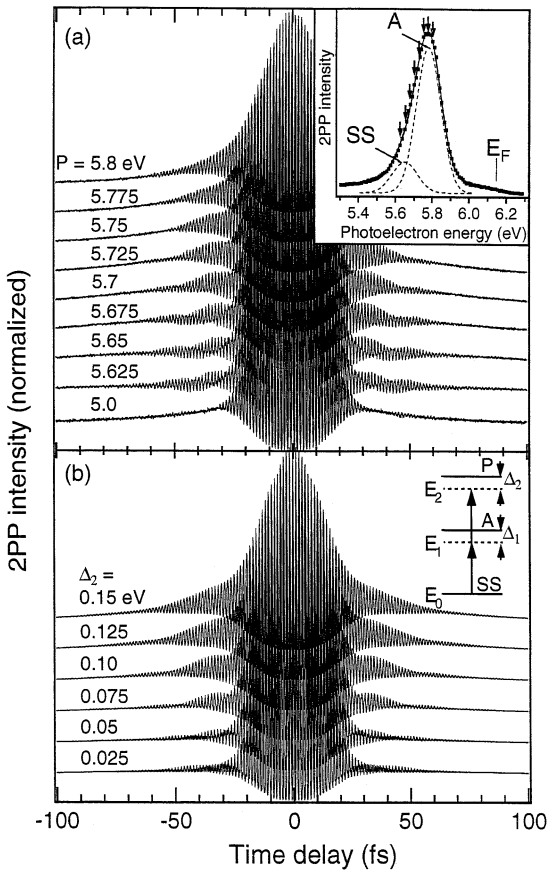

FIG. 2. (a) I2PC scans and 2PP spectrum (inset) for 0.11 ML Cs/Cu(111) at 33 K, which show long phase decay near the SS $\rightarrow A$ resonance and quantum beats. (b) Simulation based on three-level optical Bloch equations (inset).

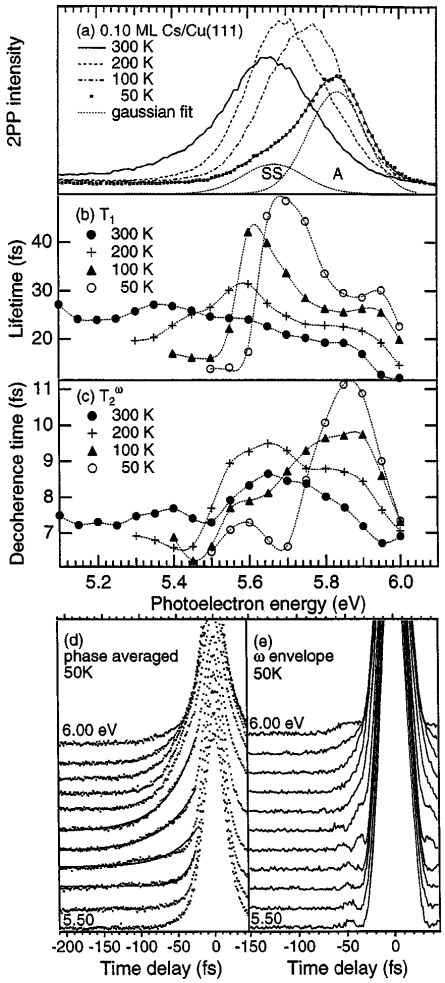

FIG. 3. (a) Temperature-dependent 2PP spectra, (b) T_1, (c) $T_2{}^{\omega}$, (d) phase averaged I2PC, and (e) ω envelopes. Solid lines in (d) are single exponential fits, which demonstrate the nonexponential decay of A.

beating) that is most prominent for energies below A. The I2PC at 5.0 eV, where the 2PP is from the bulk sp band, serves as an upper limit of the instrument response function, i.e., laser pulse autocorrelation [16]. To understand the origin of the quantum beats, the I2PC scans are simulated by optical Bloch equations (OBE), a density matrix formalism for calculating the time evolution of populations and polarizations induced by optical excitation [15,16]. The I2PC scans in Fig. 2(b) are simulated for a three-level system, which consists of SS, A, and the detected portion of the final state free-electron wave continuum P, by solving the OBE for the time-integrated population of the final state as a function of pump-probe delay. The continuous bulk contribution is neglected, since the SS and A peaks dominate the 2PP signal. For the simulation in Fig. 2(b), the laser detuning from the SS $\rightarrow A$ resonance is $\Delta_1 = 0.13$ eV, $E_0 = 0$ eV, $E_1 = \hbar\omega = A - \Delta_1$, and $E_2 = 2\hbar\omega = P - \Delta_2$. The simulation is performed with the phase and energy relaxation parameters $T_1 = 50$ fs, $T_2{}^{02} = 15$ fs, and $T_2{}^{\omega} = 15$ fs. The simulation qualitatively reproduces the dependence of quantum beats on P, which arises from the frequency difference between the driving field at ω and the system response, i.e., linear polarizations corresponding to the SS $\rightarrow A$ and $A \rightarrow P$. Experiments and simulations for different values of Δ_1 support this conclusion.

The shift of the SS $\rightarrow A$ resonance and the energy and phase relaxation times T_1 and $T_2{}^{\omega}$ [15] for 0.11 ML coverage of Cs are shown in Figs. 3(a)–3(c) ($T_2{}^{02}$ for the clean surface is discussed in Ref. [15]). As the temperature is decreased from 300 to 50 K, the SS peak position is nearly constant, but A increases from 5.4 to 5.83 eV due to both the temperature and the photodesorption shifts. At 300 K, T_1 near the SS $\rightarrow A$ resonance is enhanced by $\sim$10 fs with respect to the lifetimes of bulk sp-band hot electrons at the same energy [23], which agrees well with a value of 11 fs reported in Ref. [14]. With decreasing temperature, both T_1 and $T_2{}^{\omega}$ increase, with particularly strong changes occurring below 100 K. Experiments at different Cs coverages show that the increase in lifetimes is due to the surface temperature rather than to the energy of A with respect to the Fermi level. The phase and energy relaxation kinetics below A are noticeably nonexponential. This is due to quantum beating, and a slow incoherent component, which appears as a delayed rise. The data in Figs. 3(b) and 3(c) are obtained by forcing single exponential fits to the envelopes in Figs. 3(d) and 3(e). At 50 K, the derived values of T_1 have a maximum at 0.17 eV *below A*. The nonexponential decays and shift of the T_1 maximum with respect to A are attributed to the dissociative nuclear motion of Cs, as will be described in a future publication. During desorption, both the energy of A and coupling to the surface decrease with increasing Cu-Cs distance, resulting in a longer T_1 below the spectral maximum of A. The energy dependence of $T_2{}^{\omega}$ is also complicated, since it has contributions from the decoherence of the SS hole and A electron, which at 50 K result in two maxima. These do not coincide exactly with the SS and A peaks in Fig. 3(a) because the fits do not account for the quantum beating in Fig. 3(e). At 33 K, $T_2{}^{\omega}$ is 15 fs, which is consistent with a deconvoluted linewidth of A of 70 $\pm$ 10 meV.

The long phase and energy relaxation times for Cs/Cu(111) in Fig. 3 are unprecedented, since the linewidths of adsorbate resonances on metal surfaces imply $\ll$10 fs lifetimes. For instance, for the $2\pi^*$ derived level of CO/Cu(111), at 3.5 eV, $\hbar/\Gamma = 0.8$ fs which is in agreement with $T_1 < 5$ fs from time-resolved photoemission [6]. However, for the image potential (IP) states of copper [18], linewidths underestimate lifetimes because they are dominated by quasielastic, transverse phase relaxation [18,24]. For Cs/Cu(111), the e-h decoherence resulting in $T_2 < 2T_1$ may be induced by both the carrier-phonon scattering, which is significant due to a low Debye temperature of 60 K [11], and dissociative nuclear motion. The measured T_1 is also significantly longer than the calculated electron transfer times from the Cs $6s$, $6p$, and $5d$ states to a jellium surface ($r_s = 2$) of 0.8, 0.2, and 2 fs [8], respectively, or the experimental estimates from

Auger resonant Raman intensities of core-excited, alkali-atom-like, rare gases [4,5]. For a surface resonance these are the times for transverse delocalization of the electron from the alkali atom into the bulk; however, in the case of a surface state, the projected band gap may prevent the delocalization of the electron into the bulk if the adsorbate interaction with $k_{\|} \neq 0$ bands is weak. Electrons trapped at the surface can relax only by a longitudinal process such as e-e scattering. Lifetimes of the IP states in the L and X gaps of copper, which can exceed 100 fs, are proportional to the degree to which their wave functions penetrate into the bulk and the e-e scattering times at the same energy [18,24,25]. The surface state penetration depends on its energy and $k_{\|}$ dependent detuning from the band gap edges [26]. Although $k_{\|}$ is not defined for disordered systems such as Cs and CO on Cu(111), the vast difference in lifetimes suggests that the former bears some similarity to the IP states.

According to the density functional calculations of Ishida and Liebsch, since A is formed by the antibonding hybridization of s-p_z, optical excitation leads to a strong polarization of the electron density from the Cu-Cs bond towards the vacuum [9,10,14]. Since most of the electron density is on the vacuum side of the Cs core [10,18], the lifetime of A is dominated by the depleted electron density near the surface and the nature of the hybridization between the Cs and Cu surface. Hybridization depends on the symmetry, spatial overlap, and energy denominator between the interacting orbitals [26]. Since s and p_z orbitals are totally symmetric with respect to the surface normal, A will have the best overlap with the electron density associated with the totally symmetric SS and band edge electrons at the $L_{2'}$ point [27]; however, energy denominators for both interactions are large (>3 eV). By symmetry, Cs atoms at an atop site *cannot* hybridize with the p_x and p_y orbitals of Cu, but in hollow sites there is an additional hybridization with the p_x and p_y component of the Q_2 band, which is energetically favorable [27]. This may explain the shorter lifetimes at higher temperatures. For Cu(100) and Cu(110), the Δ_1 and Σ_1 bands, respectively, are near resonant with A [27]. Furthermore, these bands will have long tails into the vacuum providing good overlap with the s and p_z orbitals of A, since all of their kinetic energy is associated with $k_{\perp}$. Significantly, the lifetime of A is too short to resolve for Cu(100) and Cu(110) (not shown). The much shorter lifetime of CO/Cu(111) is probably due to both the shorter Cu-C bond length (1.9 Å) and symmetry of the $2\pi^*$ orbital, which can resonantly interact with the Q_2 band. Thus, the symmetry atop adsorption of Cs on Cu(111) renders the unique *surface state* character to A, which severely limits the channels for the phase and energy relaxation.

In summary, ultrafast electronic relaxation of Cs antibonding state on Cu(111) is studied by interferometric time-resolved two-photon photoemission. Both the long time scale ($T_1 = 11$ fs and $T_2{}^{\omega} = 50$ fs at 50 K) and the nonexponential behavior of the phase and energy relaxation are without precedent considering the strong interactions of chemisorbed species on metal surfaces. The nonexponential population decay is attributed to the photodesorption of Cs. The uniquely long lifetimes due to weak hybridization in the antibonding state between the Cs atom in the atop site and Cu(111) surface highlight the importance of symmetry and band structure in the electronic quenching of adsorbates. Cs/Cu(111) is an excellent system to directly probe the transition state in photodesorption, to investigate the possibility of coherent control of reactions on surfaces, and to probe the nature of chemisorption of alkali atoms on metal surfaces.

The authors acknowledge valuable discussions with Y. Murata, H. Ishida, D. Menzel, W. Worth, M. Wolf, and U. Höfer, technical support by M. Moriya, M. Matsunami, and S. Saito, and also M. Weida for critical reading of the manuscript. We also acknowledge a NEDO International Joint Research Grant for the partial funding of the project.

[1] J. W. Gadzuk, Surf. Sci. **342**, 345 (1995).
[2] D. Menzel and R. Gomer, J. Chem. Phys. **41**, 3311 (1964).
[3] P. A. Redhead, Can. J. Phys. **42**, 886 (1964).
[4] A. Sandell *et al.,* Phys. Rev. Lett. **78**, 4994 (1997).
[5] C. Keller *et al.,* Phys. Rev. Lett. **80**, 1774 (1998).
[6] L. Bartels *et al.,* Phys. Rev. Lett. **80**, 2004 (1998).
[7] A. M. Bradshaw, H. P. Bonzel, and G. Ertl, *Physics and Chemistry of Alkali Metal Adsorption* (Elsevier, Amsterdam, 1989).
[8] P. Nordlander and J. C. Tully, Phys. Rev. B **42**, 5564 (1990).
[9] H. Ishida, Phys. Rev. B **38**, 8006 (1988).
[10] H. Ishida and A. Liebsch, Phys. Rev. B **45**, 6171 (1992).
[11] S. Å. Lindgren *et al.,* Phys. Rev. B **28**, 6707 (1983).
[12] D. A. Arena, F. G. Curti, and R. A. Bartynski, Phys. Rev. B **56**, 15 404 (1997).
[13] N. Fischer *et al.,* Surf. Sci. **314**, 89 (1994).
[14] M. Bauer, S. Pawlik, and M. Aeschlimann, Phys. Rev. B **55**, 10 040 (1997).
[15] S. Ogawa *et al.,* Phys. Rev. Lett. **78**, 1339 (1997).
[16] H. Petek and S. Ogawa, Prog. Surf. Sci. **56**, 239 (1997).
[17] S. Å. Lindgren and L. Walldén, Phys. Rev. B **45**, 6345 (1992).
[18] E. Knoesel, A. Hotzel, and M. Wolf, J. Electron Spectrosc. Relat. Phenom. **88–91**, 577 (1998).
[19] M. Bauer, S. Pawlik, and M. Aeschlimann, Surf. Sci. **377–379**, 350 (1997).
[20] D. L. Adler *et al.,* Phys. Rev. B **48**, 17 445 (1993).
[21] In addition, Φ and A increase due to possible adsorption of impurities and the presence of defects, which makes it difficult to quantify the pure photoinduced effect.
[22] B. Hellsing *et al.,* J. Chem. Phys. **106**, 982 (1996).
[23] S. Ogawa, H. Nagano, and H. Petek, Phys. Rev. B **55**, 10 869 (1997).
[24] U. Höfer *et al.,* Science **277**, 1480 (1997).
[25] E. V. Chulkov *et al.,* Phys. Rev. Lett. **80**, 4947 (1998).
[26] J. W. Gadzuk, Surf. Sci. **43**, 44 (1974).
[27] H. Eckardt, L. Fritsche, and J. Noffke, J. Phys. F **14**, 97 (1984).